Polarization of the Recoil Proton from π^0 Photoproduction in Hydrogen*

J. O. MALOY AND V. Z. PETERSON†
California Institute of Technology, Pasadena, California

AND

G. A. SALANDIN AND F. WALDNER
Istituto di Fisica dell'Università, Padova, Italy and Istituto Nazionale di Fisica Nucleare, Sezione di Padova, Italy

AND

A. MANFREDINI
Istituto di Fisica dell'Università and Istituto Nazionale di Fisica Nucleare, Sezione di Roma, Italy

AND

J. I. FRIEDMAN‡ AND H. KENDALL‡
W. W. Hansen Laboratories of Physics, Stanford University, Palo Alto, California

(Received 18 May 1964; revised manuscript received 19 April 1965)

The polarization of the recoil proton in neutral single-pion photoproduction from hydrogen, $\gamma+p \rightarrow p+\pi^0$, has been measured for pion center-of-mass angles near 90° at 7 photon energies from 450 to 900 MeV. The polarization rises to a maximum of 0.58 near 600 MeV and is still 0.42 at 900 MeV. The sign of the polarization is negative in the sense of $\mathbf{k}\times\mathbf{q}$, where $\mathbf{k}$ is the photon momentum and $\mathbf{q}$ is the pion momentum. The measured values are given as functions of laboratory photon energy and c.m. pion angle as follows: 450 MeV, 109°, -0.16 ± 0.14; 525 MeV, 84°, -0.36 ± 0.19; 585 MeV, 86°, -0.58 ± 0.15; 660 MeV, 77°, -0.51 ± 0.17; 755 MeV, 76°, -0.55 ± 0.15; 810 MeV, 89°, -0.45 ± 0.17; 895 MeV, 90°, -0.42 ± 0.16. The recoil protons were momentum-analyzed with a magnetic spectrometer. Nuclear emulsion was used as scatterer and detector. The emulsion technique is discussed in detail. The number of individual scatterings in emulsion used for each measurement varied between 750 and 1000.

I. INTRODUCTION

An accurate measure of the polarization of the recoil proton in the reaction $\gamma+p \rightarrow p+\pi^\circ$ was first obtained by P. C. Stein at Cornell, who found large polarizations at 90° in the c.m. system for laboratory photon energies of 500 and 700 MeV.[1] Because polarization at 90° c.m. can only occur when two states of opposite parity interfere, his results have been taken as good evidence that the parity of the second resonance is odd, opposite to the parity of the first resonance. The direction of polarization was negative in the sense $\mathbf{k}\times\mathbf{q}$, where $\mathbf{k}$ is the photon momentum and $\mathbf{q}$ the pion momentum, as predicted by Peierls[2] from the behavior of the angular distribution.

More extensive measurements, using a counter technique similar to that of Stein, were made at Frascati and have been reported by Querzoli, Salvini, and Silverman,[3] and by Mencucinni, Querzoli, and Salvini.[4] A bubble-chamber measurement was reported by the Pisa group.[5]

A full understanding of the second resonance, the nonresonant terms in both π^0 and π^+ production, and the nature of the third and higher resonances will require much more detailed measurements of both differential cross sections and polarizations. The present experiment was undertaken with the intention of making a systematic set of measurements of the polarization near 90° c.m. for photon energies both above and below the second resonance, using a qualitatively different technique.

In a previous paper,[6] we have described measurements of the polarization of the recoil proton from the photoproduction reaction $\gamma+p \rightarrow p+\pi^0$ at center-of-mass angles near 90° and at three photon energies near the second resonance at 1.55 GeV total center-of-mass energy. The polarization of the recoil proton was determined by a measurement of the scattering asymmetry in nuclear emulsion. The three measurements reported previously were based upon a total of 2500 scattering events. Four new measurements have been made, and the final results of all seven measurements, based on a total of 5900 scattering events, are given in the present paper.

Transverse polarization of a proton beam is measured

* This work was supported in part by the U. S. Atomic Energy Commission, the U. S. Office of Naval Research, and the Italian Committee for Nuclear Research (C.N.R.N.).

† Present address: University of Hawaii, Honolulu, Hawaii.

‡ Present address: Massachusetts Institute of Technology, Cambridge, Massachusetts.

[1] P. C. Stein, Phys. Rev. Letters **3**, 473 (1959); see also P. L. Connolly and R. Weill, Bull. Am. Phys. Soc. **4**, 23 (1959).

[2] R. F. Peierls, Phys. Rev. Letters **1**, 174 (1958); Phys. Rev. **118**, 325 (1960).

[3] R. Querzoli, G. Salvini, and A. Silverman, Nuovo Cimento **19**, 57 (1961).

[4] C. Mencuccini, R. Querzoli, and G. Salvini, Phys. Rev. **126**, 1181 (1962).

[5] L. Bertanza, P. Franzini, I. Manelli, G. V. Silvestrini, and V. Z. Peterson, Nuovo Cimento **19**, 952 (1961).

[6] J. O. Maloy, G. A. Salandin, A. Manfredini, V. Z. Peterson, J. I. Friedman, and H. Kendall, Phys. Rev. **122**, 1338 (1961).

by scattering the beam from some material and observing the degree of asymmetry of the elastic scattering in the plane normal to the direction of polarization. Because a scattering is necessary, the integrated beam intensity must be much higher than that needed to measure a cross section with comparable accuracy.

Scattering of polarized protons with large inelastic energy losses (30 MeV or more) tends to be symmetric, so that it is necessary to define the energy of the proton beam incident upon the analyzer to an accuracy which allows one to reject highly inelastic events. The lighter elements, such as carbon, are excellent polarization analyzers for protons with energies of 120 MeV or more. By choosing a heavier element as the analyzer, one can reduce the relative amount of inelastic scattering at the cost of reduced analyzing power. It follows that the appropriate choice of the analyzing material depends to some extent on the attainable energy resolution.

The elastic-scattering cross sections are rapidly varying functions of angle, so that it is important that there be no inherent asymmetry in the experimental apparatus if spurious asymmetries are to be avoided. Because the number of recoil protons is a function of the laboratory angle of the recoil, inherent asymmetries are introduced when a finite scatterer is placed between finite detectors, even if the alignment of the apparatus is perfect. To avoid the experimental compromise which must be made between this effect and the need for a finite counting rate, we used nuclear emulsion as scatterer and detector, so that the scattering angles could be directly measured. The analyzing power of emulsion at the energies of interest has been measured as a function of energy and angle. The data will be discussed in Sec. IV.

The observed polarization of the recoil proton beam is the mean of the polarizations of the protons from all contributing processes, weighted by the relative yields of each process. To obtain the polarization of the recoil proton from the reaction $\gamma+p \rightarrow p+\pi^0$, one must know the relative yield and the polarization of the protons from any important competing processes. One cannot tolerate appreciable background, even in known amounts, from reactions which produce protons of unknown polarization. In all but one of our exposures we avoided accepting many protons from such poorly understood processes as multiple pion production. We have tolerated background protons from a process (electron scattering) whose polarization and yield we can compute.

II. EXPOSURES

A plan view of the experimental arrangement is shown in Fig. 1. The energy-analyzed and focused high-energy electron beam of the Stanford Mark III linear accelerator impinged upon a copper radiator placed $2\frac{1}{2}$ in. in front of a liquid-hydrogen target. In the early runs, the radiator was 0.011 in. thick; in the later runs, it was

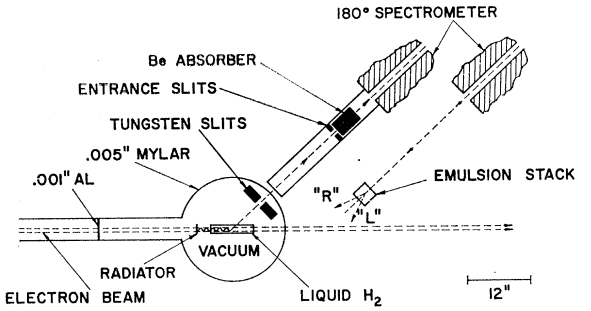

FIG. 1. Plan view of the experimental arrangement. The tungsten slits shown were used with the 72-in. spectrometer only, and the absorber was used only in the highest energy runs (U,AA, AB).

0.116 in. thick. The target cell was 8 in. long, 1 in. in diameter, and had 1.2-mil stainless-steel end windows. The bremsstrahlung produced in the radiator traversed the target together with the electron beam. The electron beam was allowed to pass through the hydrogen because it proved impossible to deflect it without extensive modification of the existing target and radiator assembly. Recoil protons from the irradiated hydrogen target were magnetically analyzed and focused on the emulsion stack using one of the two vertically-bending double-focusing 180° magnetic spectrometers constructed by the Hofstadter group.[7,8] The 36-in. spectrometer was used in the early runs, and the 72-in. instrument was used in the later high-energy runs. The use of vertical bending meant that allowance had to be made for precession of the proton moment in the magnet, as shown in Fig. 2. This point is discussed below.

The protons were collimated by lead entrance slits about 30 in. from the target. In later runs, beryllium absorbers were placed behind the slits to slow the protons, for reasons to be discussed further on. During these runs, additional apertures were placed near the target and inside the spectrometer to reduce the degradation of the angular resolution as a result of scattering in the absorber. The slit jaws near the target were made of tungsten, and were movable. Their opening subtended an angle of about 7 deg. at a distance of about $7\frac{1}{2}$ in. from the target center.

Ilford G-5 pellicles, 400 and 600 μ thick, were used in most of the runs; K-5 sensitivity was used in a few runs. The pellicles were aligned with stainless-steel pins passing through precision-punched holes. The front end of the stack was smoothed to facilitate accurate range measurements. A millimeter grid, also aligned with the steel pins, was printed on each pellicle for position location and ease in tracing tracks between pellicles. The emulsion stack assembly, consisting of about 60 pellicles clamped between aluminum blocks,

[7] R. Hofstadter, Rev. Mod. Phys. **28**, 214 (1956).
[8] F. Bumiller, M. Crossiaux, E. Dally, and R. Hofstadter, Phys. Rev. **124**, 1623 (1961).

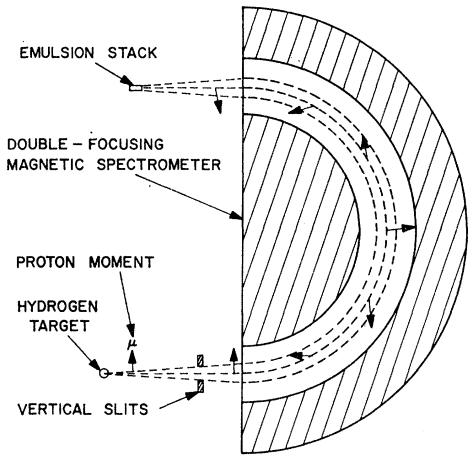

FIG. 2. Precessional motion of the proton magnetic moment in passing through the spectrometer.

was placed near the exit focus. The stack was oriented by a keyed holder and leveled so that the plane of the pellicles was horizontal, to ensure maximum track length in emulsion, and to make it possible to use the dip of a track as a measure of the total bending angle of the proton.

Table I lists the exposure conditions for the 9 runs

TABLE I. Exposure conditions.

Run	Electron-beam energy (MeV)	Proton angle (deg)	Proton energy (MeV)	Proton energy (MeV)	Radiator thickness (inches)	Electron charge (μC)
B	600	33.0	139	450	0.011	2000
C	650	43.5	143	···[a]	0.011	380
D	700	47.7	143	660	0.011	3000
E	580	39.0	143	525	0.011	4200
F	650	43.5	143	585	0.011	2400
U	870	40.9	256[b]	825	0.116	3680
V	840	48.0	170	755	0.116	1905
AA	880	40.0	256[b]	805	0.116	7150
AB	950	40.6	285[a]	895	0.116	13 580

[a] Empty-target run.
[b] Beryllium absorbers were used to reduce proton energy to 170 MeV in the spectrometer.

made and analyzed. Runs B, C, D, E, and F were made with the 36-in. spectrometer; runs U, V, AA, and AB used the 72-in. spectrometer. Results from runs B, D, and F were given in our earlier report.[6] In the earlier runs with the 36-in. spectrometer the angular resolution in the production plane was defined by the horizontal entrance aperture and the pole faces of the magnet, while the resolution in azimuthal angle was essentially defined by the vertical aperture, since the beam height was small. In the later runs, the desired angular resolution was obtained by placing the additional apertures mentioned above near the target and inside the spectrometer. The tungsten slits inside the target chamber were aligned optically, and their position was checked by observing the cutoff in the proton flux when the slits were moved to various angles.

The measured dispersions of the large and small spectrometers are 0.35 and 0.70% per in., respectively. The variations in mean momentum across the emulsion stacks, about $1\frac{1}{2}$ in. thick, were, respectively, about 3 and 6 MeV/c. Aberrations and finite-source size caused momentum spread at any point of the image of about 5 and 10 MeV/c, respectively.

The proton momentum resolution was sufficiently narrow that the photon energy resolution was almost completely determined by the angular resolution of the system. Except in the 450 MeV run (run B), the angular resolution and peak bremsstrahlung energy were chosen to discriminate strongly against recoil protons from multiple pion production.

Because the magnetic field of the vertically-bending spectrometers was normal to the plane containing the magnetic moment of the proton, the moment precessed about the field lines, as shown in Fig. 2. The moment precession angle is related to the total bending angle of the linear momentum of the proton by the formula $\Omega=\delta[1+(\mu-1)E/M]$, where $\mu-1=1.79275$ (the anomalous moment in nuclear magnetons) and E/M is the total energy of the proton in units of the rest energy. The numerical values for Ω/δ are 3.062 at 540 MeV/c and 3.118 at 590 MeV/c, so that in our exposures the magnetic moment precessed slightly more than one and a half turns when the central momentum vector was deflected through half a turn (180 deg). Hence, the principal effect of the precession was to reverse the direction of polarization. At the exit from the magnet the angle between the moment and the vertical was 12 deg at 540 MeV/c, and 21 deg at 590 MeV/c. The maximum fractional reduction in the observable component of the polarization on the central ray was $[1-\cos(21°)]$, or 7.6%.

The precession was different for different orbits. The finite spread in entering dip angles (at most ± 3.3 degrees) accepted by the entrance slits resulted in a spread in the angles between the proton moment and the vertical at the exit of the spectrometer. The variation about the central value was ± 19 deg in the worst case. Using the relation between the precession along each track and the dip angle at the exit of the spectrometer, we estimated the position of the moment for each scattering event.

To hold the scanning conditions constant, a single value of the proton momentum was used for an entire series of runs. A lower limit on the momentum used was set by the fact that the analyzing power of emulsion falls off at energies below 150 MeV. An upper limit was set by the precession of the proton moment, which increases with energy and leads to an appreciable reduction in the transverse component of the polarization. During the earlier runs, only the 36-in. spectrometer was available, and it was used at the maximum momentum it could focus without saturation, 540 MeV/c, or

144-MeV kinetic energy. In these runs, the spectrometer was used without an absorber, so that the pion center-of-mass angle could not be held constant, but varied between 77 and 109 deg. The 72-in. spectrometer was available for the later runs, and a higher proton momentum of 590 MeV/c (170 MeV) was used to obtain a longer useful track length in emulsion. In three runs beryllium absorbers were used to slow the protons to this value, and in these runs it was possible to hold the pion center-of-mass angle constant near 90 deg.

Background from the empty target was measured in various ways. One exposure (run C) was made with the target empty, and the emulsion was scanned. In all runs except run B, the empty-target background was also measured using a counter arrangement in place of the emulsion stack. Protons were counted with the target full and empty, and with the entrance slits open and closed. At first this counting was done with a single counter, and an appreciable counting rate remained even with the slits closed, which presumably resulted from neutron-capture gamma rays in the shielding. Subtraction yielded an estimate of the empty target background. In the latest runs, a two-counter telescope was placed above the emulsion stack assembly to measure background and to provide a continuous monitor of the counting rate. Pulse-height analysis was used to separate the protons from the gamma-ray background. In some runs, additional lead shielding was required in front of the spectrometer to shield the entrance aperture from the radiator. The empty-target backgrounds, which were typically about 5% of the full-target yields, are tabulated with the final results in Table II.

The electron beam intensity was a strong function of the machine energy and the tuning, but was typically 300–500 μC per h. The charge was integrated with a secondary emission monitor which was calibrated for each run with a Faraday cup. The Faraday cup itself was not used as a monitor during the runs because scattering in the radiator caused some of the electrons to miss the cup.

TABLE II. Observed scattering asymmetries and polarizations uncorrected for background.

Run	Scan method	Useful scatters R	Useful scatters L	Polarization, %[a] Without inelastic correction	Polarization, %[a] With inelastic correction
B	Area	504	471	−14±12	−15±13
D	Follow	142	80	−78±22	−88±24
	Trace-back	138	117	−24±17	−27±18
	Area	368	273	−54±14	−58±15
	Combined[b]	470	367	−36±12	−39±13
E	Follow	305	244	−29±16	−32±17
F	Area	533	436	−49±13	−51±13
U	Follow	63	51		
AA	Follow	341	305		
U+AA	Combined	404	356	−37±14	−40±15
V	Area	542	420	−42±12	−48±13
AB	Area	451	364	−35±13	−37±14

[a] Uncorrected values were computed using the solid analyzing power curves in Fig. 4. Corrected values were computed using the dashed curves.
[b] Duplications eliminated.

III. SCANNING

The flux of collimated protons (±1.3 deg in projected angle, ±5 deg in dip) was readily distinguished from pre-exposure background protons. In runs D, which was typical, noncollimated tracks averaged 20 per plate of 465 good tracks. Pion tracks were nearly at minimum ionization and could not be confused with proton tracks.

Obviously inelastic events, such as stars with 2 or more prongs, including p-p scatters, or events with visible recoils or with Auger electrons were easily detected and eliminated. A few recoil proton tracks were observed at random angles.

The scanning methods used were: (a) *area scanning*, in which overlapping fields of view were systematically searched for scattering events; (b) *track following*, in which the protons were followed along the track from a line near the incident edge until a scattering event was observed or the track went out; (c) *trace back*, in which the tracks making an angle of 4.5 deg or more with the mean proton direction at a depth of a centimeter were traced back toward the incident edge to distinguish between single, plural, and multiple scattering events. The scanning was done at the nuclear emulsion laboratories at Padua (track following), Rome (trace back, and later track following) and CalTech (area scanning).

The area scanning method proved to be the most rapid, with an average counting rate for the best stack of 1.1 scattering events per observer hour. The results of duplicate scanning showed that practiced observers could detect scattering with projected angle change between 3 and 20 deg with an efficiency of about 80%.

The optimum proton density for area scanning was determined by experience to be about 8000 protons/cm^2. Compromises had to be made in running time so that intensities in some exposures were as low as 2000 protons/cm^2, which decreased the counting rate. The density in one exposure (run B) was 15 000 protons/cm^2. This density produced the highest counting rate, but the scanning was more laborious.

The track-following method was the slowest, but is well known to be efficient in detecting scatterings as small as 2 deg. The Padua group obtained measures of the mean free path for elastic and inelastic scattering, which were used to compute the correction for inelastic scattering described later.

The trace-back method is efficient in detecting scattering along a given track, but the selection of wide angle tracks resulted in the loss of a number of events because of multiple scattering toward smaller angles of tracks on which single scatters had occurred. The efficiency can be increased at the cost of a decrease in

the counting rate, which is limited by the large number of multiply scattered tracks which must be followed for each single scattering detected. This method was used only on part of one stack (run D).

The numbers of events found using each of the various methods are given in Table II. Most of the events, 71%, were found by area scanning, while 25% were found by track following, and 4% by the trace-back method.

When a scattering event was detected, the scanners sketched the event, and measured the projected angle and the dip of the track before and after scattering, as well as the value of the nearest grid coordinate. The projected angles were measured with an uncertainty of ± 0.3 deg, and the dips with an uncertainty of at most 1.0 deg in unprocessed emulsion. Measurements of the dip near the edge of the emulsion were corrected for distortion. The projected angle measurements on each plate were referred to the emulsion grid. The grids printed on the pellicles were aligned within about 0.1 deg, so that the angular measurements in different pellicles could be compared and an absolute mean direction established. Events were recorded which satisfied criteria placed on the direction of the track before scattering and on the magnitude of the scattering angles. The criteria were different for each method and are listed in Table III.

TABLE III. Selection criteria.

Method	Initial projected angle	Initial dip	Projected angle change	Dip-angle change
Track following	$\leq 5°$[a]	$\leq 5°$[a]	3–20°	All
Trace back	4.5°–25°[a]	$\leq 25°$[a]	6–20°	0–20°
Area scan	$\leq 8°$	$\leq 10°$	3–20°	0–20°

[a] At depth at which track was selected for following.

The length of track scanned varied with the method, but was at most 23 mm in the low-energy exposures and at most 30 mm in the high-energy runs.

A number of precautions were taken to avoid the introduction of left-right bias arising from a difference in the efficiencies for the detection of scatterings of opposite signs. During the area scan, the use of a reticle was avoided in searching for scatters; angular measurements were done separately. The trace-back method is subject to spurious asymmetry if the angular cutoffs to left and right are biased to one side. Comparison of the numbers of multiple-scattered tracks to left and right proved to be a sensitive measure of the alignment, and showed that the residual misalignment was at most 0.1 deg. From an estimate of the sensitivity of the trace-back method to an angular misalignment, we found that the spurious asymmetry introduced in the trace-back data was at most 1%.

In the four later runs (U, V, AA, AB) every other pellicle in each stack was reversed during the exposure, then turned over for scanning, so that any residual scanning bias averaged out. For a sample of 824 events found by area scanning the left-right ratio was 375/449 when the reversal was allowed for, but 409/415 when it was not. The bias indicated by this ratio is $0.72 \pm 3.5\%$, a value which is certainly consistent with zero.

Duplicate scanning, by different observers in a single group or by different groups, was also used to establish the absence of left-right bias in each scanning method. The efficiencies for the detection of left and right scattering were measured separately and compared. On run F, the area scanning method was found to be $(81 \pm 3)\%$ efficient in detecting scattering to the left from 3 to 20 deg in projected angle, while the efficiency for detecting scattering to the right was $(84 \pm 3)\%$. The bias, the difference in the efficiencies divided by their sum, was therefore $2 \pm 3\%$. This value is again consistent with zero. Similar results with similar statistical errors were obtained for the other stacks and from the intercomparison of the different scanning methods. We conclude that there is no evidence of left-right bias in any of our detection procedures. At worst, the uncertainty in the final polarization values resulting from undetectable residual bias is now thought to be 5% or less in the absolute value. The upper limit of 10% quoted in our earlier paper was based on fewer measurements.

IV. ANALYZING POWER OF NUCLEAR EMULSION

The differential cross section for scattering of protons with polarization P as a function of scattering angle θ and kinetic energy T may be written as

$$\sigma(\theta,T)=\sigma_0(\theta,T)[1+\alpha(\theta,T)P\cos\phi],$$

where ϕ is the angle between the proton spin and the normal to the scattering plane, $\alpha(\theta)$ is the analyzing power of the scattering material, and σ_0 is the differential cross section averaged over ϕ. The scattering of protons from carbon, silver, and most other elements in the range of angles and proton energies of interest here is such that protons tend to scatter in the direction $\boldsymbol{\mu} \times \mathbf{p}$, where $\boldsymbol{\mu}$ is the proton magnetic moment vector and $\mathbf{p}$ is the proton momentum. Protons with spin up tend to scatter to the left. Following the usual convention,[9] we have taken the sign of the polarization to be positive when scattering to the left predominates.

The variation of $\alpha(\theta)$ with scattering angle for protons of 135 MeV is shown in Fig. 3 for carbon, silver and for nuclear emulsion. The C and Ag curves are smooth fits to cyclotron data of Dickson and Salter,[10] for elastic scattering only, excluding the 4.4-MeV and higher levels of carbon. Assuming that all of the heavy elements in emulsion scatter like silver, and that all

[9] L. Wolfenstein, Ann. Rev. Nucl. Sci. **6**, 66 (1956).
[10] J. M. Dickson and D. C. Salter, Nuovo Cimento **6**, 235 (1957).

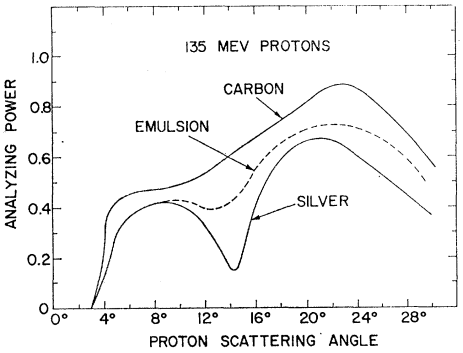

FIG. 3. Analyzing power of 135-MeV polarized protous in carbon, silver, and nuclear emulsion. The curves for carbon and silver are taken from the data of Dickson and Salter (Ref. 10). The curve for nuclear emulsion is a weighted average of the data for carbon and silver, assuming that the light and heavy elements in emulsion have the same scattering asymmetry as carbon and silver, respectively.

of the light elements scatter like carbon, we have constructed the expected analyzing-power curve for normal Ilford G-5 emulsion, shown by the dotted line. Data are also available at 95-, 155-, 170-, 185-, and 220-MeV for a variety of elements.[11] It is reasonable to expect that one can synthesize an accurate analyzing power curve for emulsion from the constituent elements, because the observed scattering asymmetries are smooth functions of atomic number. The scattering from silver dominates at small angles, but the scattering from carbon in emulsion fills in the dip at the diffraction minimum that would otherwise be observed for silver.

Verification that such a synthesis is accurate is provided by the measurements of J. G. Rutherglen, who measured the analyzing power of emulsion directly using the Harwell proton-scattering polarization apparatus at proton energies of 143, 115, and 91 MeV.[12] We consider his results, shown in Fig. 4, to be a definitive calibration of emulsion at these energies and we have relied on a synthesis at higher energies.[13]

The analyzing power is a function of the excitation energy of the residual nucleus. The early cyclotron measurements from carbon showed high polarization values whenever the energy resolution was narrowed.[14] Measurements made at Uppsala show that the analyzing power decreases almost linearly with ΔE, the excitation energy.[15] The largest scattering asymmetry occurs for $\Delta E=0$ (elastic scattering) while at $\Delta E=30$ MeV the asymmetry is comparable with the low value observed at these energies in nucleon-nucleon scattering. This dependence holds approximately true for a wide variety of elements. The polarizations in elastic scattering are somewhat higher for light elements, but this advantage is largely lost if the energy resolution is not narrow, since the light elements have relatively strong excited levels in the energy interval levels in the 10–50 MeV. In Fig. 5, we have plotted our estimates of the analyzing power of emulsion and of carbon for two values of the experimental resolution, 0 and 30 MeV.

The effect of lowered analyzing power is to require a larger number of events in order to achieve the same absolute uncertainty in the proton *polarization*. The number of events required varies inversely as the square of the analyzing power. Up to a certain point it is better to accept some inelastic events to increase the counting rate if their polarization continues to be high; for carbon, the low-lying levels at 4.4 and 9.6 MeV have high polarization at somewhat larger angles than the peak in the elastic polarization. Plots of $\alpha^2(\theta)\sin\theta$ for emulsion using various energy resolutions show that the use of 30-MeV energy resolution provides enough additional scattering events to make up for lost analyzing power, but that inclusion of events with 50-MeV loss increases the error in a polarization measurement despite the increase in the number of events.

A systematic program to measure the inelasticities of scattering in emulsion was undertaken at Padua. Other work was done on a smaller scale at Rome and CalTech. Since the incident proton energy was very well defined, the energy loss in scattering could easily

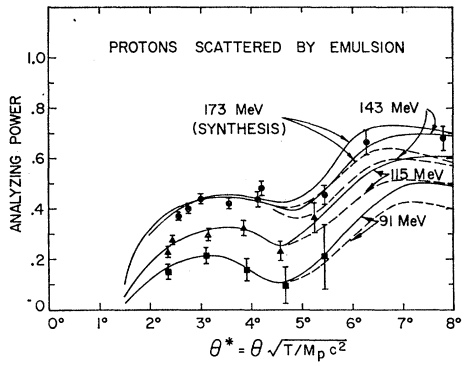

FIG. 4. Analyzing power of polarized protons in nuclear emulsion. The measurements are those of Rutherglen (Ref. 12). The 91-, 115-, and 145-MeV solid curves are fits to the data. The silver and carbon data were used at very small and very large angles, respectively, to establish the shape of the curves. The 173-MeV curve has been calculated using the extrapolation procedure described in the text. The dashed curves show the analyzing power after correction for the larger energy losses accepted during scanning.

[11] A critical review of the literature for measured scattering asymmetries of protons from various elements, for both elastic and inelastic scattering, has been made by one of us (V.Z.P.). Copies of a bibliography and a summary of results including curves for normal, 2× and 4× dilute emulsion are available upon request.

[12] J. G. Rutherglen, Proc. Phys. Soc. (London) **76**, 427 (1960).

[13] The cyclotron data are sufficiently detailed and consistent that we did not complete an effort to determine the analyzing power of emulsion, using pellicles which were exposed to the polarized proton beam of the Harvard cyclotron through the kindness of Richard Wilson.

[14] J. M. Dickson, B. Rose, and D. C. Salter, Proc. Phys. Soc. (London) **68**, 361 (1955).

[15] A. Johansson, G. Tibell, and P. Hillman, Nucl. Phys. **11**, 540 (1959).

be determined by measuring the range of the scattered proton. In this way the energy loss could be determined within about ± 5 MeV. Figure 6(a) shows the energy loss distribution of scatters found in along-the-track scanning at Padua. The ratio of events with 30 to 140 MeV loss to those with 0 to 30 MeV loss was $25/58=0.43$ for this sample, which included wide-angle events whose space scattering angle was greater than 20 deg. Most of these events were not obviously inelastic, that is, were not stars or events with Auger electrons. Figure 6(b) shows the scattering angle distribution of elastic and inelastic events in the range 5 to 20 deg. All three scanning groups also grain-counted the tracks before and after scattering to determine the energy loss. By counting 300 grains before and after scattering, it proved possible to measure the energy loss in scattering with an uncertainty of about ± 10 MeV.

Using these measurements, we established that a trained scanner could detect scattering with an energy loss greater than about 30 MeV by inspection from the change in grain density. The scanners were asked to record all events found, including those thought to be inelastic. Energy-loss measurements were subsequently made on some of these events. Some results are shown in Figs. 7(a) and 7(b). In these histograms, those events which the scanners rejected as inelastic are represented by dark rectangles. Only two events with an energy loss greater than 30 MeV had been accepted, while 18 had been rejected. On the other hand, only one event with an energy loss less than 30 MeV had been rejected. These results were obtained from area scan data, but also apply to the track-following method. The energy resolution of the trace-back method was narrower than 30 MeV, since the inelastically scattered tracks had lost more energy at the depth from which they were followed, with the result that the contrast between a slowed track and its neighbors was increased.

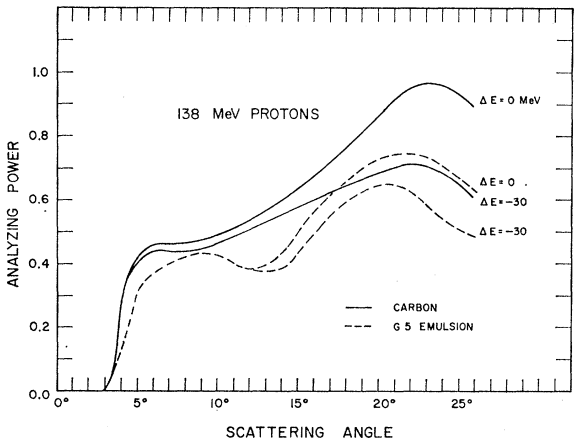

FIG. 5. Elastic and inelastic scattering asymmetry in nuclear emulsion. The inelastic scattering asymmetry was calculated by assuming that the inelastic scattering is uniformly distributed in energy loss and angle, and that only those inelastic events with energy loss less than 30 MeV were accepted. The magnitude of inelastic scattering relative to elastic scattering was estimated from the data given in Fig. 6.

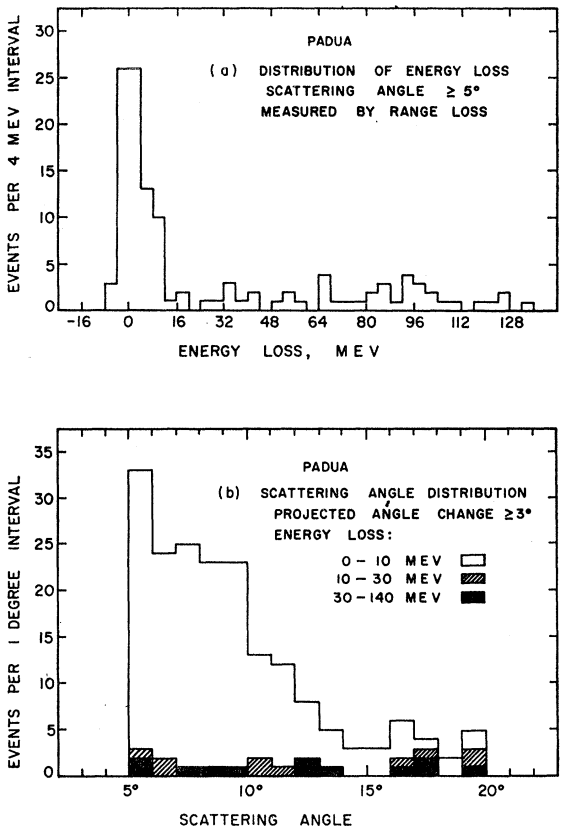

FIG. 6. Distributions in energy loss and angle of elastic and inelastic scattering of protons in nuclear emulsion. The incident proton energy was 144 MeV, and the tracks were followed until the energy had dropped to 130 MeV. (a) Energy-loss distribution of events with space scattering angle greater than 5 deg. (b) Angular distributions as a function of energy loss of events with projected scattering angle greater than 3 deg.

Before computing the polarization, a correction was applied to the analyzing power at wide angles to take account of the greater proportion of inelastic scattering accepted in our scanning, relative to the high-resolution cyclotron experiments. The correction to the analyzing power was computed by assuming that the analyzing power decreases linearly to zero at an energy loss ΔE_0, and that the energy spectrum consists of a quasi-elastic peak, with $\Delta E \leq 10$ MeV, and a uniform inelastic spectrum of events excluded in the cyclotron measurements. Under these assumptions, the corrected analyzing power $\bar{\alpha}(\theta)$ is given in terms of the uncorrected analyzing power $\alpha_0(\theta)$ by the relation

$$\bar{\alpha}(\theta)=\alpha_0(\theta)\left[1-\frac{1}{2}\frac{\sigma_i(\theta)\Delta E_m^2/\Delta E_0}{\sigma_0(\theta)+\sigma_i(\theta)\Delta E_m}\right].$$

In this formula, $\sigma_0(\theta)$ is the strength of the quasi-elastic peak and $\sigma_i(\theta)$ is the magnitude of the inelastic scattering per unit energy loss, in arbitrary but con-

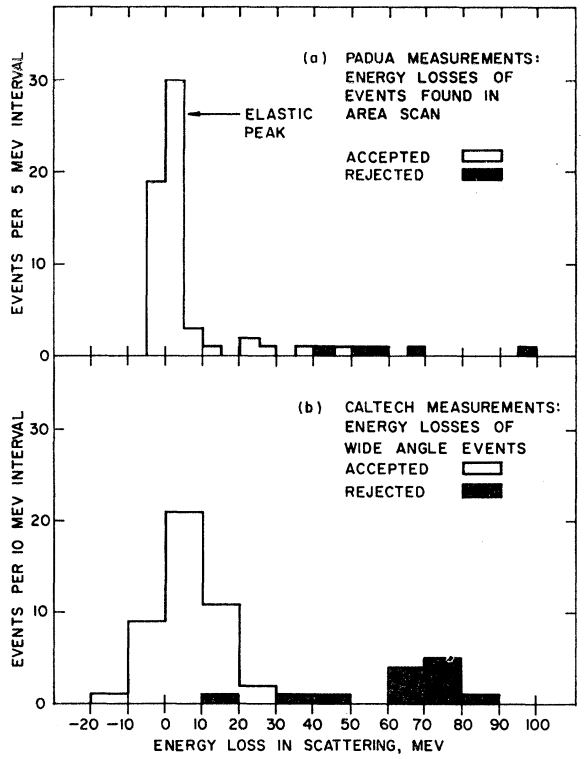

FIG. 7. Classification of run D events accepted by scanners as elastic, or rejected as inelastic (black squares) according to the measured energy loss. (a) Using Padua range loss measurements. (b) Using CalTech measurements of grain density change.

sistent units. The energy ΔE_m is the largest energy loss accepted in the scanning procedure. Both ΔE_0 and ΔE_m were taken to be 30 MeV. The values of the yields σ_0 and σ_i were estimated from the Padua measurements shown in Fig. 6(b). The inelastic scattering was assumed to be independent of angle.

To obtain the dependence of the analyzing power on proton energy, we assumed that the inelastic yields remain constant while the elastic cross-section decreases with energy. The elastic cross-sections are known with some accuracy for the range of energies considered here, and measurements of the inelastic yields at 96 MeV[16] and 185 MeV[17] show small differences.

The values of the analyzing power used in the polarization computation are shown as smooth curves in Fig. 4, as functions of energy and the angular variable $\theta^*=\theta(T/M_pc^2)^{\frac{1}{2}}$ (T=kinetic energy, M_pc^2=proton rest energy, θ=space scattering angle.)

V. ANALYSIS OF EMULSION DATA

The results of scanning the eight emulsion stacks, to obtain between 750 and 1000 scattering events at each photon energy, are summarized in Table II. In this table, we have listed the numbers of scatterings to the left (L) and to the right (R) and the polarizations obtained. The polarization values have not yet been corrected for background.

The polarization was computed by use of the maximum-likelihood method. Each scattering event was considered as a single sampling of the three-dimensional distribution

$$f(\theta,\phi,T;P)=N\epsilon(\theta,\phi,T)\sigma_0(\theta,T)[1+\alpha(\theta,T)P\cos\phi].$$

The symbols are defined as follows: The random variables are the space scattering angle θ, the azimuthal angle ϕ and the kinetic energy T. The functions are the unpolarized scattering cross section σ_0, the analyzing power α, and the detection efficiency ϵ, assumed to be unbiased in that the detection is not correlated with $\cos\phi$. The polarization P is the parameter to be determined, while N is a normalization factor, which does not depend on P if the efficiency is unbiased.

The likelihood function of an entire sample of n events (θ_i,ϕ_i,T_i), $i=1,\cdots n$, is then

$$L=\prod_{i=1}^{n} f(\theta_i,\phi_i,T_i;P).$$

The values of the random variables θ, $\cos\phi$, and T were computed for each event from the projected angles and the depth in emulsion of the scattering events. The emulsion range-energy data of Barkas *et al.* was used.[18,19]

The value of P corresponding to the maximum of the likelihood function was obtained numerically. When computed as a function of P, the likelihood was found to differ from a Gaussian curve by at most 1 or 2% in all cases. The rms width of the likelihood function has been taken as an estimate of the error in the polarization.

In Figs. 8 and 9 are shown some typical distributions of space scattering angle θ and the value of $\cos\phi$. Figure 8 shows typical scattering angle distributions obtained from the area scanning and the trace-back scan. Data from the track-following method have already been presented in Fig. 6(b). When the distributions of azimuthal angles accepted by the different scan procedures are taken into account, the histograms agree well with expectations from the known cross sections for scattering by the elements in emulsion. The dependence of the scattering asymmetry on $\cos\phi$ shows plainly in Fig. 9, where we have plotted the contribution of left and right scattering separately using the area scan data from run D. The geometrical constraints are responsible for the gross shape of the histogram.

The distribution of the proton energy before scattering of accepted events was approximately uniform, to 10%, between the limits of 112 and 144 MeV for the

[16] K. Strauch and F. Titus, Phys. Rev. **103**, 200 (1956).
[17] H. Tyrén and A. J. Maris, Nucl. Phys. **3**, 52 (1957).
[18] W. H. Barkas, Paul H. Barrett, Pierre Cüer, H. H. Heckman, F. M. Smith and H. Ticho, UCRL 3768, 1957 (unpublished).
[19] W. H. Barkas, UCRL 3769, 1957 (unpublished).

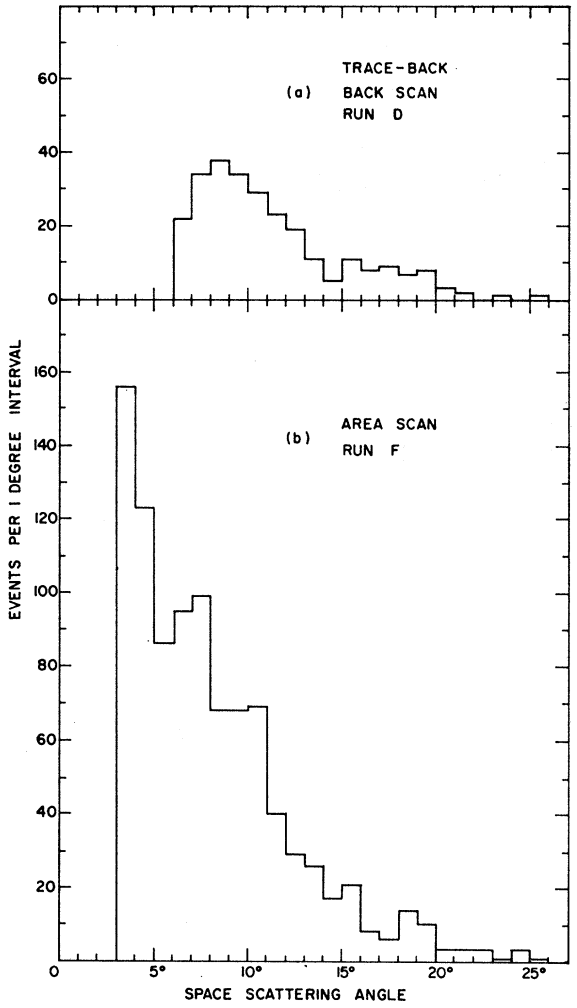

FIG. 8. Distribution in space scattering obtained with different scanning techniques. (a) Method of tracing back tracks making an angle greater than 4.5° with the main flux at a depth of 23 mm. (b) Method of area scanning for events scattering with projected angle change greater than 3 deg. Refer to Fig. 6 for similar results obtained by following tracks.

low-energy runs and 125 and 170 MeV for the high-energy runs. In run D, the track following data covered the interval 130 to 144 MeV.

All valid events detected in the scanning, except those whose scattering angle was larger than about 20 deg, were included in the final analysis, even if the space scattering angle was as small as 3 deg and the cosine of the azimuthal angle was nearly zero. Since each of the less significant events was assigned an appropriately small weight by the maximum likelihood procedure, their inclusion did not dilute the sample. Checks of the validity of this procedure were made by recomputing the polarization for run D, restricting the space angle to values larger than 5 deg, and the absolute value of $\cos\phi$ to values larger than 0.707. The recomputed polarization differed by only 4%, and the statistical uncertainty $\sigma(P)$ increased by the expected amount. For purposes of computation, the smooth curves in Fig. 4 were represented in tabular form. Linear interpolation in energy was used.

The polarizations were computed using both the analyzing power obtained from the cyclotron measurements, and the analyzing power corrected for inelastic scattering as described previously. Both functions are shown in Fig. 4. The difference in the polarizations obtained from the two calculations was, at most, 10%, indicating that inelastic scattering is not an important source of uncertainty in an emulsion measurement of polarization in the range of energies used. Both the corrected and uncorrected values are listed in Table II.

In the area scan, there was a small probability, at most 3%, that the polarization of a scattered proton had been reduced by a previous single scattering. During the data analysis, an additional uniform constraint was placed on the projected angle and dip before scattering, which assured that most of the scattered tracks accepted for analysis had previously undergone only multiple scattering. No correction has been applied for the residual double scattering contribution.

Because the measurements made to detect left-right scanning bias gave no evidence that significant bias existed, we have made no correction for bias. In the later runs, in which the pellicles were alternately flipped over, any residual bias should have been averaged out.

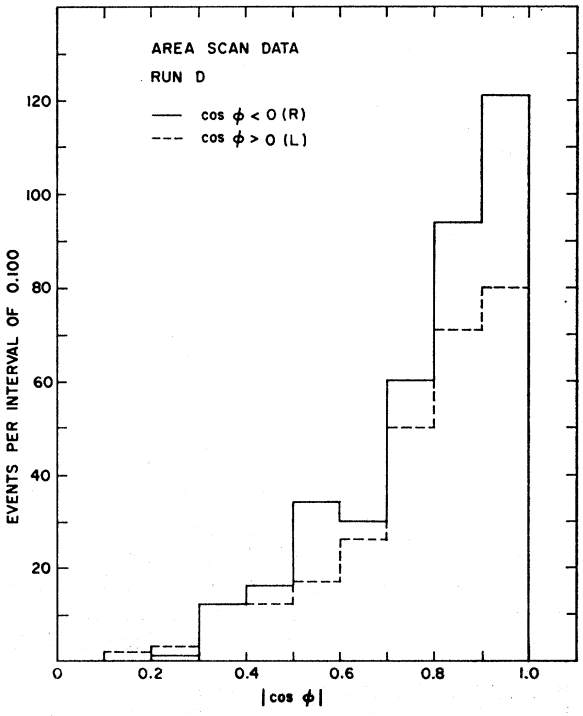

FIG. 9. Distribution of the cosine of the azimuthal angle of scattering, observed in run D (39% polarization), plotted separately for scattering to the left and right.

Accordingly, the polarizations corrected for inelastic scattering, given in the last column of Table II, are taken to be the polarizations of the protons which were accepted by the spectrometer. They have not yet been corrected for unpolarized background.

VI. BACKGROUND CORRECTIONS

Background protons were produced by photoproduction and electron scattering in the target walls, as well as by certain processes competing with single π^0 photoproduction. Because the electron beam passed through the hydrogen target, the yields from certain electron interactions were significant. The competing processes were

(1) elastic electron scattering by electrons which had lost energy in the radiator

$$e^-+A \rightarrow e^-+A+\gamma, \quad \text{(bremsstrahlung)}$$

followed by elastic electron scattering

$$e^-+p \rightarrow e^-+p.$$

(2) Inelastic scattering with photon emission

$$e^-+p \rightarrow e^-+p+\gamma.$$

(3) Direct electron production (electroproduction) of pions

$$e^-+p \rightarrow e^-+p+\pi^0.$$

(4) Double pion production

$$\text{(a)}\ \gamma+p \rightarrow p+\pi^+ +\pi^-,$$
$$\text{(b)}\ \gamma+p \rightarrow p+\pi^0+\pi^0.$$

Recoil protons from processes (1) and (2) are unpolarized, as one can show by a direct electrodynamic calculation from the Feynman diagrams for these processes.

The cross section for elastic scattering of electrons on protons has of course been thoroughly measured.[8] The cross section for the radiative scattering, $e^-+p \rightarrow e^-+p+\gamma$, has been estimated theoretically by Schiff.[20]

In our background calculations, we used Schiff's formula for the cross section, in the form quoted by Tautfest and Panofsky in their paper describing a measurement of the effect.[21] A more recent calculation, by Maximon and Isabelle,[22] shows that when the incident electron energy is 200 MeV the approximations made by Schiff produce a result which is high by as much as 40% at low energy, if the electron scattering angle is in the range 30–150° and the incident electron loses half its energy or more. We estimate that the Schiff cross section is high by at most 20% under the conditions of our exposures. The corresponding difference in the total number of pions produced is only about 2%, so that we have not repeated the calculations.

The yields were computed by an IBM 7090 Monte Carlo program, which also determined the resolution of the magnet and its apertures, taking into account multiple scattering in the beryllium absorber used in some of the later runs. The energy distribution of the electrons was calculated using the approximate Bethe-Heitler thick-target spectrum.[23] The bremsstrahlung spectrum was taken from the calculations made at Stanford by Alvarez,[24] which were also based on the Bethe-Heitler spectrum. The ratio of values of the two spectra should be quite accurate. The electron-scattering cross sections were calculated from the form factors given by Bumiller *et al.*,[8] while the cross sections for the photoproduction of neutral pions were taken from the data of Diebold.[25]

Since only the ratio of the electron-scattering and photopion yields was required, the uncertainty of the calculation should be comparable to the uncertainty in the ratio of the experimental cross sections (about 20%).

The same program was used to verify that in most runs the aperture was set to discriminate against recoil protons from multiple pion production. In the calculation, the angular distribution of the multiple pions was taken as the distribution in phase space, normalized to the values of the total cross section for the reaction $\gamma+p \rightarrow p+\pi^+ +\pi^-$ measured by Chasan, Cocconi, Cocconi, Schechtman, and White.[26] In all runs except run B, the multiple pion yield calculated in this way was less than 1% of the single pion yield because recoil protons from multiple pion production were kinematically forbidden over most or all of the aperture. In run B, the electron-beam energy was set well above the double-pion threshold, so that an appreciable number of recoil protons from this process were accepted. For this run, we have estimated the double-pion contribution from the data of Richter, who has measured the recoil proton yield at 36.45° in the laboratory as a function of electron-beam energy, using the same equipment and the same proton momentum as we did.[27] Our run B was made at a laboratory angle of 33.0 deg, and at a beam energy of 600 MeV, 46 MeV above the 554-MeV threshold for double π° production. At the slightly larger angle used by Richter, the threshold is 30 MeV higher, or 585 MeV. At an energy 46 MeV above this threshold (630 MeV), the recoil proton yield measured by Richter has increased by about 5% as a result of the double pion processes. We conclude that this contribution produces a systematic uncertainty of *at most* 6% in the value of

[20] L. I. Schiff, Phys. Rev. **87**, 750 (1952).
[21] G. W. Tautfest and W. K. H. Panofsky, Phys. Rev. **105**, 1356 (1957).
[22] L. C. Maximon and D. B. Isabelle, Phys. Rev. **133**, B1344 (1964).
[23] H. A. Bethe and W. Heitler, Proc. Roc. Soc. **A146**, 83 (1934).
[24] R. A. Alvarez, Jr., Stanford High Energy Physics Laboratory Internal Memorandum HEPL-228, 1961 (unpublished).
[25] R. Diebold, Phys. Rev. **130**, 2089 (1963).
[26] B. M. Chasan, G. Cocconi, V. T. Cocconi, R. M. Schectman, and D. H. White, Phys. Rev. **119**, 811 (1960).
[27] Burton Richter, Phys. Rev. Letters **9**, 217 (1962).

TABLE IV. Resolutions, backgrounds, and final polarization values.

Run	Lab. photon energy (MeV)	Photon energy resolution (MeV)[a]	c.m. pion angle	c.m. angular resolution*	Backgrounds relative to total $1\pi^\circ$ yield (nearest percent) $e^-+p\rightarrow e^-+p$	$e^-+p\rightarrow e^-+p+\gamma$	$\gamma+p\rightarrow p+2\pi$	$e^-+p\rightarrow e^-+p+\pi^0$	Empty target	Corrected polarization (%)
B	450	30	109°	8°	0.004	0.002	0.05	0.46	0.03	-16 ± 14
E	525	35	84°	5°	0.04	0.02	0	0.38	0.05	-36 ± 19
F	585	50	86°	8°	0.06	0.04	$<1\times10^{-4}$	0.39	0.05	-58 ± 15
D	660	65	77°	7°	0.15	0.11	0	0.36	0.05	-51 ± 17
V	755	70	76°	6°	0.06	0.01	$<2\times10^{-4}$	0.06	0.07	-55 ± 15
U,AA	825,805 (Av. 810)	75	90°	7°	0.04	0.01	<0.005	0.07	0.08	-45 ± 17
AB	895	85	90°	8°	0.07	0.01	<0.005	0.06	0.05	-51 ± 16

[a] Full width at half-maximum, to nearest 5 MeV and 1°, respectively.

the polarization at 450 MeV; the maximum error would be obtained only if the protons from double pion production were completely polarized in the direction opposite to that observed.

Electroproduction with small momentum transfer (small angular deflection of the incident electron) is highly favored. For such small momentum transfers, the electroproduction process is essentially equivalent to bremsstrahlung followed by photoproduction, and the yield may be calculated to a good approximation by treating the contribution from the process as if it were equivalent to an increase in the thickness of the physical radiator.[28] The correction for the finite range of momentum transfer to the three-body final state is of approximately the same size and character as the correction for the finite thickness of the equivalent real radiator, typically 0.02 radiation lengths. Differences between the details of the two processes thus correspond to differences in the detailed shape of the photon-energy resolution, as long as the electroproduction process involves only transversely polarized vitrual photons. For the earlier runs (B, D, E, F), the radiator used was quite thin, so that the contribution of electroproduction was substantial, as much as 45%. We therefore investigated the contribution of those terms in the electroproduction amplitude which would give rise to polarization different from photoproduction, namely, those terms corresponding to longitudinal polarizaton of the virtual photon appearing in the Feynman diagram of the electroproduction process.

These terms were integrated over the electroproduction phase space, assuming that the production amplitudes appearing were constant in energy and angle. As a result of these calculations, we estimate that the contribution of such terms to the total proton yield cannot exceed 5%, or else their effect would have been observed in the experiment of Panofsky and Allton.[29] We have therefore treated the electroproduction as it if were equivalent to photoproduction in calculating the pion yield. The radiation length used in the calculations was the sum of the effective radiation length for electropion production and the radiation length of all other material in the beam, including hydrogen.

Empty target background increased with radiator thickness, presumably as a result of multiple scattering of the electron beam in the radiator. We have taken this effect as evidence that the background originated mainly from electron scattering in the target walls, and therefore have assigned zero polarization to this component of the total yield.

The results of the background and resolution calculation are given in Table IV, in which we have listed the estimated relative yields of the recoil protons from the various background processes. We believe these estimates to be accurate to about 20%. The final corrected values of the polarization are given in the last column of the table. The new values for runs B, D, and F, obtained after applying the background correction calculated by the computer, are only slightly different from the values given in our previous paper.[6]

VII. DISCUSSION

Our results, together with those obtained at Cornell and Frascati, are plotted against laboratory photon energy in Fig. 10. The different measurements appear to be quite consistent. The polarization is slowly varying over the entire energy region from 600 to 900 MeV, indicating an appreciable interference between photoproduction amplitudes of opposite parity.

The shape of the π^0 angular distribution near the maximum at 1.55-GeV c.m. is roughly fitted by $5\text{-}3\cos^2\theta$, indicating that the predominant state has an angular momentum $J=\frac{3}{2}$, and is excited by dipole radiation. This conclusion was originally drawn by R. R. Wilson.[30] The third maximum at 1.7 GeV seems to involve interaction with a total angular momentum of at least $\frac{5}{2}$.[31,32] It is difficult to decide whether the exciting radiation is quadrupole, octupole or a mixture, since the angular distributions have a similar shape in either case.

[28] R. H. Dalitz and D. R. Yennie, Phys. Rev. **105**, 1598 (1957).
[29] W. K. H. Panofsky and E. A. Allton, Phys. Rev. **110**, 1155 (1958).
[30] R. R. Wilson, Phys. Rev. **110**, 1212 (1958).
[31] F. P. Dixon and R. L. Walker, Phys. Rev. Letters **1**, 142 (1958).
[32] J. I. Shonle, Phys. Rev. Letters **5**, 156 (1960).

Different level schemes were proposed in efforts to explain the observed maxima by resonance models. The schemes which have been seriously discussed are the following:

Author	Level	Total angular momentum	Orbital angular momentum	Parity	Exciting multipole (lowest order)
Wilson (30)	II	$\frac{3}{2}$	1	Even	Magnetic dipole
Peierls (2)	II	$\frac{3}{2}$	2	Odd	Electric dipole
	III	$\frac{5}{2}$	3	Even	Electric dipole
Landovitz, Marshall (37)	II	$\frac{3}{2}$	1	Even	Magnetic dipole
	III	$\frac{3}{2}$ or $\frac{5}{2}$	2	Odd	Electric dipole, magnetic quadrupole

In each scheme the first level (the 3-3 resonance, or N^*) has total angular momentum $\frac{3}{2}$ and even parity.

It is not to be expected that such simple models can explain the data in detail, since the fourth state at 1.9-GeV c.m. has been omitted, and nonresonant amplitudes are certainly present. Still, we may expect to narrow the field of choice by eliminating those models which disagree violently with the data.

The original motivation for the various polarization experiments, including the present one, was a suggestion by Sakurai.[33] He pointed out that if the first and second states had opposite parity, one might expect a large polarization at 90° in the center of mass system at energies between the resonances. Such a large polarization is in fact observed, and the sign is consistent with the sign of the forward-backward asymmetry in the angular distribution.

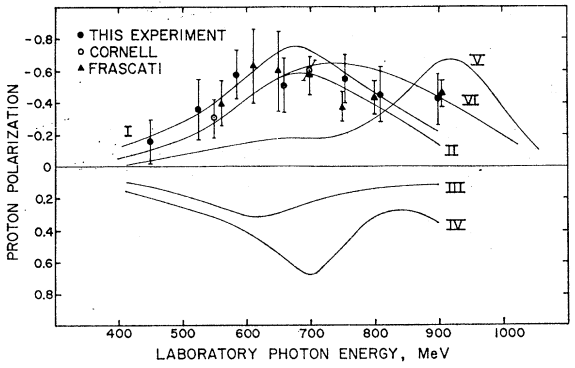

FIG. 10. Final polarization values and results of model calculations. Model calculations have been made by fitting one level resonance formulas (with barrier factor) to the total cross sections at the three resonances, choosing the sign of the amplitudes to agree with the sign of the interferences observed in the angular distributions. The magnetic dipole, $j=\frac{3}{2}$ amplitude from the first resonance was included in all models. The other multipoles present in each model are given in the following table (E or M implies electric or magnetic radiation, respectively; $j\gamma$=photon angular momentum, J=total angular momentum, and l=orbital angular momentum of final state). Nonresonant s waves were added to the models indicated.

Model	Resonance energy (GeV) c.m.[a]	Resonant multipole E/M	$j\gamma$	j	l	Parity	S wave added?
I	1.55	E	1	$\frac{3}{2}$	2	−	No
II	1.55	E	1	$\frac{3}{2}$	2	−	Yes
III	1.55	M	1	$\frac{3}{2}$	1	+	Yes
IV	1.55	M	1	$\frac{3}{2}$	1	+	Yes
	1.74	M	2	$\frac{5}{2}$	2	−	
V	1.55	M	1	$\frac{3}{2}$	1	+	Yes
	1.74	M	2	$\frac{3}{2}$	2	−	
VI	1.55	E	1	$\frac{3}{2}$	2	−	Yes
	1.74	E	2	$\frac{5}{2}$	3	+	

[a] These energies were given incorrectly in our previous paper (Ref. 6).

Stoppini and Pelligrini suggested that the polarization might in fact be produced even if the second state were magnetic dipole, if nonresonant S waves were present.[34] An investigation of this proposal showed, however, that the predicted polarization is smaller than that observed, having an upper limit of $1/\sqrt{10}=0.316$. Furthermore, the sign of the polarization is inconsistent with the sign of the asymmetry in the angular distribution.[35] On the other hand, if the second resonance is odd-parity (electric dipole), the presence of S waves decreases the polarization slightly to provide better agreement of the model with the data. The argument is given in detail by Pelligrini and Stoppini in a later paper.[36]

L. F. Landovitz and L. Marshall suggested that the polarization observed at energies below the second resonance might actually arise from interference between the first and the third resonances.[37] In such a model the second resonance would be P wave, magnetic dipole M_{1+}, while the third would necessarily be D wave. This suggestion has been discussed in detail elsewhere.[35] Four possible choices for the higher state were examined: electric dipole (E_{2-}) or a magnetic quadrupole (M_{2-}), with total angular momentum $\frac{3}{2}$; magnetic quadrlpole (M_{2+}) an electric octupole (E_{2+}) with total angular momentum $\frac{5}{2}$. (The notation for the multipoles is that of Chew, Goldberger, Low and Nambu[38]; the letter indicates the type of radiation (electric or magnetic), the numerical subscript in-

[33] J. J. Sakurai, Phys. Rev. Letters **1**, 258 (1958).

[34] G. Stoppini and C. Pellegrini, *Proceedings of the Ninth International Conference on High-Energy Physics, Kiev, 1959* (Academy of Science, USSR, 1960).

[35] J. O. Maloy, Ph.D. thesis, California Institute of Technology, 1961 (unpublished).

[36] C. Pellegrini and G. Stoppini, Nuovo Cimento **17**, 269 (1960).

[37] L. F. Landovitz and L. Marshall, Phys. Rev. Letters **3**, 190 (1959).

[38] G. F. Chew, M. L. Goldberger, F. E. Low, and Y. Nambu, Phys. Rev. **106**, 1354 (1957).

dicates the orbital angular momentum of the final state, and the sign indicates the j value: $j=l+\frac{1}{2}$ or $l-\frac{1}{2}$). The inteference of M_{1+} and E_{2+} can be eliminated at once since the maximum polarization can be shown to be $\frac{1}{10}\sqrt{2}=0.141$. We can also exclude the electric dipole amplitude, since the angular distribution near the third resonance seems to be completely inconsistent with production by dipole radiation. The other two possibilities were examined by making crude numerical fits to the data, deriving the three resonant amplitudes and phases from a one-level resonance formula of the kind used successfully to fit the total cross section near the first resonance by Gell-Mann and Watson.[39] Centrifugal barrier factors were included in the scattering widths. The widths and normalizations were adjusted to fit the total cross sections for π^--p scattering and π^0 photoproduction, respectively.

Only neutral-pion photoproduction was considered, to avoid complication from the meson-current term in charged photoproduction. The first resonance was assumed to be magnetic-dipole $P_{3/2}$, with a resonance energy of 1.2 GeV c.m. The reduced width was 58 MeV. The second resonance was located near 1.55 GeV; the resonance energy was adjusted for those models in which interference shifted the peak in the total cross section. The reduced width varied between 22 and 30 MeV, depending on the angular momentum. The third resonance was located at 1.74 GeV. A constant nonresonant S-wave amplitude, corresponding to a cross section of 0.3 μb/sr, was included in some calculations. The magnitude and sign were chosen to fit the forward-backward asymmetry in the angular distribution in the region of the first resonance; the amplitude is almost certainly too large at high energy. The formulas and the parameters of the resonant amplitudes used are given in detail elsewhere.[35]

The polarization computed using various models is plotted, with the experimental results, in Fig. 10. To obtain the cross section and polarization, the complex amplitudes derived from the one-level formula were substituted in the multipole expansion of the photoproduction cross section given by Chew, Goldberger, Low, and Nambu.[38] These curves (except for VI) are the same as those given in our earlier paper.[6] The only plausible choice for the second-state amplitude appears to be electric dipole, D-wave, with total angular momentum $\frac{3}{2}$. The assumption that the third state is $J=\frac{5}{2}$, magnetic quadrupole, (M_{2-}) produces a large polarization, but there is again an inconsistency between the sign of the polarization and of the forward-backward asymmetry in the angular distribution, which is quite negative about the second resonance, a result well confirmed by numerous measurements[25,40,41] From this analysis, we conclude that the parity of the second resonance must be odd if the large, negative polarizations are to be *simply* explained.

We cannot make so strong a statement regarding the third resonance, since our measurements extend only to 900 MeV. However, we are able to produce agreement with our data if the third resonance is taken to be even parity, $F_{5/2}$, electric quadrupole, as shown by the curve VI in Fig. 10. A similar conclusion has also been reached by the Frascati group.[3,4] The sign of the polarization is consistent with that of the asymmetry in the angular distribution. This analysis is not, of course, a rigorous multipole analysis in the sense that the multipoles present have been determined by quantitative goodness-of-fit tests.

Quantitative fits of simple models have been attempted, by Kilner[42] and Diebold, in particular, and have been unsuccessful. Diebold's attempts are described in his paper.[25]

Kilner attempted to fit the π^+, π^+/π^-, and π^0 data simultaneously using a mixture of Born approximation terms, vector meson pole terms, and multipoles, using charge independence to relate the various reactions. Although plausible curves were produced, the criteria of goodness-of-fit were never well satisfied. Systematic discrepancies between the data of different laboratories are partly to blame, but the principal difficulty is a different one. The Born terms, in particular the meson-current term, contribute strongly to charged pion photoproduction, but there is little evidence of the unmodified Born terms in neutral pion photoproduction. This problem has been discussed by Höhler, Dietz, and Müllenseifen,[43] and by Salin,[44] who have presented qualitative fits to the cross-section and polarization data using modifications in the Born approximation. Höhler, Dietz, and Müllensiefen suggest that the polarization of the recoil nucleon may be explained by interference of a P-wave resonance with the electric Born amplitude. Since this amplitude consists primarily of S waves, we believe that the argument given above (involving the sign) eliminates this possibility. Salin finds that it is necessary to include nonresonant $P_{1/2}$ waves (M_{1-}) in the π^0 amplitude to achieve a good fit above 500 MeV. We have not included these in our analysis.

VIII. CONCLUSION

The measured values of the polarization of the recoil proton in neutral pion photoproduction, $\gamma+p\rightarrow p+\pi^0$, have been listed in Table IV. Our analysis of these data

[39] M. Gell-Mann and K. M. Watson, Ann. Rev. Nucl. Sci. 4, 219 (1954).
[40] R. Talman, Ph.D. thesis, California Institute of Technology, 1962 (unpublished).
[41] G. Bellettini, C. Bemporad, and P. L. Braccini, Nuovo Cimento **29**, 1195 (1963).
[42] J. R. Kilner, Ph.D. thesis, California Institute of Technology, 1963 (unpublished).
[43] G. Höhler, K. Dietz, and A. Müllensiefen, Nuovo Cimento **21**, 186 (1961).
[44] P. Salin, Nuovo Cimento **28**, 1294 (1963).

leads us to prefer the following assignment of quantum numbers to the three lowest pion-nucleon resonances:

State	J	l	Wave	Parity	Radiation
I	$\frac{3}{2}$	1	P	Even	Magnetic dipole
II	$\frac{3}{2}$	2	D	Odd	Electric dipole
III	$\frac{5}{2}$	3	F	Even	Electric quadrupole

ACKNOWLEDGMENTS

This experiment was instituted as a collaboration between members of the Synchrotron Laboratory at CalTech and the High Energy Physics Laboratory at Stanford, and we wish to acknowledge the encouragement and support provided by R. F. Bacher at CalTech and W. K. H. Panofsky at Stanford in carrying out this program. We also wish to thank R. Hofstadter for his cooperation in the use of the magnetic spectrometers developed under his direction.

Part of the work done in Italy was completed while one of us (V. Z. P.) was in residence in Rome as a Research Scholar under Fulbright Fellowship and a Guggenheim travel grant.

Numerical computations were performed with the Burroughs 220 and IBM 7090 computers at the CalTech Computing Center.

The exposures were succesfully performed only through the unrelenting efforts of the Stanford linear accelerator beam operators and technicians to obtain maximum beam energy and intensity.

Finally, the actual data are the direct result of skilled and consistent work on the part of the scanning teams at Padua, Rome and CalTech. In particular, we wish to thank Mrs. Elaine Motta, Mrs. Cheryl Maloy, Mrs. Nancy Gross, Mrs. Hana Elter, Mrs. Nerys Wright, and Mrs. Anna Snively.

PHYSICAL REVIEW VOLUME 139, NUMBER 3B 9 AUGUST 1965

Composite Models and $SU(6)$ Invariance*

T. K. Kuo
Brookhaven National Laboratory, Upton, New York
AND
L. A. Radicati
Scuola Normale Superiore, Pisa, Italy
(Received 30 March 1965)

In this paper we discuss a nonrelativistic model for the baryons and the baryon resonances based on three quarks with fractional charges. It is shown that it is possible to have the ground state to correspond to the 56-dimensional representation of $SU(6)$ by introducing attractive three-body forces on which are superimposed weaker repulsive two-body forces. The departure from the $SU(6)$-symmetrical limit is discussed in terms of three types of exchange forces which turn out to be of the same order of magnitude.

I. INTRODUCTION

COMPOSITE models of elementary particles have often been discussed in connection with the unitary and higher symmetries.[1–6] In the Gell-Mann–Zweig[1,2] model, the baryon $J=\frac{1}{2}^+$ octet and the $J=\frac{3}{2}^+$ decuplet are assumed to be composed of three quarks with spin $\frac{1}{2}$, fractional charge and baryon number. These quarks transform under $SU(3)$ like the three-dimensional representation. Gürsey, Lee, and Nauenberg,[3,4] on the other hand, to avoid the appearance of fractional charges, assumed that the baryon octet and decuplet are composed either of two fermion triplets or of a fermion triplet and a boson singlet.

In both models the forces which are responsible for the binding are assumed to be invariant under $SU(3)$, the degeneracy between the different members of the unitary multiplets being removed by weaker symmetry-breaking interactions.

Within the framework of these composite models, the success of the mass formulas resulting from $SU(6)$ invariance[7–11] could be explained by introducing the further assumption that the forces between quarks are predominantly independent of their spins. In this formulation the assumption is, of course, only meaning-

* Work performed under the auspices of the U. S. Atomic Energy Commission.
[1] M. Gell-Mann, Phys. Letters **8**, 214 (1964).
[2] G. Zweig, CERN report (unpublished).
[3] F. Gürsey, T. D. Lee, and M. Nauenberg, Phys. Rev. **135**, B467 (1964).
[4] T. D. Lee, Nuovo Cimento (to be published).
[5] H. Bacry, J. Nuyts, and L. Van Hove, Phys. Letters **9**, 279 (1964); **12**, 285 (1964).
[6] D. Amati, H. Bacry, J. Nuyts, and J. Prentki, CERN report (unpublished).
[7] F. Gürsey and L. A. Radicati, Phys. Rev. Letters **13**, 173 (1964).
[8] B. Sakita, Phys. Rev. **136**, B1756 (1964).
[9] A. Pais, Phys. Rev. Letters **13**, 175 (1964).
[10] T. K. Kuo and T. Yao, Phys. Rev. Letters **13**, 415 (1964).
[11] B. Bég and V. Singh, Phys. Rev. Letters **13**, 418, 509 (1964).